ABUAD Journal of Engineering Research and Development (AJERD)
ISSN (online): 2645-2685; ISSN (print): 2756-6811

Volume 6, Issue 1, 1-12

# Dynamic Performance of a Hybrid Synchronous Machine with Ultra-High $X_D/X_Q$ Ratio

Linus Uchechukwu ANIH[1], Eugene Okenna AGBACHI[2], Emeka Simon OBE[1]

[1]*Department of Electrical Engineering, University of Nigeria, Nsukka, Enugu State Nigeria*
linus.anih@unn.edu.ng, simon.obe@unn.edu.ng

[2]*Department of Electrical and Electronics Engineering, Federal University of Technology, Minna, Niger State, Nigeria*
euokenna@futminna.edu.ng

*Corresponding Author:* euokenna@futminna.edu.ng, +2348036610256

*Date Submitted:* 19/07/2022
*Date Accepted:* 18/11/2022
*Date Published:* 13/04/2023

***Abstract:*** *This paper presents a hybrid synchronous machine with ultra-high $X_D/X_Q$ ratio. A conventional synchronous machine has two components of output power; the excitation and the reluctance component. The reluctance power which depends on the saliency ratio ($X_D/X_Q$) is negligible when compared with the excitation component. A hybrid machine with variable $X_D/X_Q$ ratio has the capability of raising the reluctance component of the power to infinity theoretically. The stator frame of the hybrid machine is stacked with two identical cylindrical cores (A, B) that are magnetically isolated. A hybridised rotor; salient cum cylindrical is used. There are two windings on the stator core stacks identifiable as the main and control windings respectively which are electrically isolated but magnetically coupled. The main windings are connected in series across the two stacks (A and B) and the terminals connected to the utility supply for motor operation while for generator, the terminals feed the load busbar. The control windings are transposed in passing from one stack to the other and terminated across a balanced adjustable capacitor bank. It is shown that the quadrature axis reactance $(X_Q)$ of the hybrid machine can be adjusted from zero to infinity $(0 \le X_Q \le \infty)$ theoretically by varying the balanced adjustable capacitor bank. The reluctance component of the output power of the machine which depends on the reactance ratio $(X_D/X_Q)$ is also seen to theoretically increase to infinity. The reluctance power is shown to be twice the excitation power when the capacitor $800\mu F$ is connected to the control winding. Depending on the value of the capacitive reactance, the reluctance power can be made even ten times the excitation power.*
.

***Keywords:*** *Hybrid machine, hybridised rotor, main and control windings, magnetically isolated stacks, transposed winding*

## 1. INTRODUCTION

A conventional salient-pole synchronous machine has two components of output power, the excitation and the synchronous power components. The reluctance component is usually very small and sometimes negligible in comparison with the excitation component, in which if the reluctance power component can be made twice the excitation component, could triple the unit power of a typical synchronous machine. This low reluctance component of the output power is predicated on the low saliency $(X_d/X_q)$ ratio of a typical salient-pole synchronous machine. In general terms, to achieve high reluctance output power and power factor, it is necessary for the direct axis reactance $X_d$ to be made as large as possible while the quadrature axis reactance $X_q$ is made as small as possible. The optimum conditions for this to occur is when the salient-pole arc is very small, about one-fifth of the pole-pitch, but for such proportions, the magnetizing current becomes excessive (even in the absence of saturation) and the pull-in power falls to a very low value[1].
Various researchers have investigated different rotor configurations in the attempt to increase $X_d/X_q$ ratio [2]–[4] through manipulation of rotor geometry. The search for the most optimal rotor structure is still on. A novel strategy for increasing the saliency ratio of a synchronous reluctance machine whose output power depends wholly on the saliency ratio was introduced [5]. In this, a cylindrical rotor and a primitive salient-pole rotor machine element are mechanically coupled and

ISSN (online): 2645-2685; ISSN (print): 2756-6811

integrally wound. In this arrangement, there is no winding in the rotor of either machine element (that is, there is no field or damper windings). The major demerit of this machine is that the cylindrical machine element does not produce any output power since there is no field winding. Its function is merely to provide a synchronous reactance $X_s$ which is matched to the direct axis reactance $X_d$ of the primitive salient-pole machine element.

Agbachi et al [6], [7] adapted this approach to a conventional synchronous machine in which field and damper windings are introduced in the rotor of the two machine halves. The performance was shown to be excellent in terms of efficiency and power factor. The output power was shown to be more than thrice that of a single machine element.
The demerit of this is that the machine is bulky due to the coupling of the two machine halves. In this present study, the two machine elements are now configured as a unit machine with the field and damper windings in the rotor circuit. The machine is now having a hybrid rotor in a double stack stator core.

## 2. MATERIALS AND METHODS

The physical configuration of the machine is as shown in figure 1. In appearance, the machine is similar to the conventional synchronous machine. The major unorthodox features of the machine are:

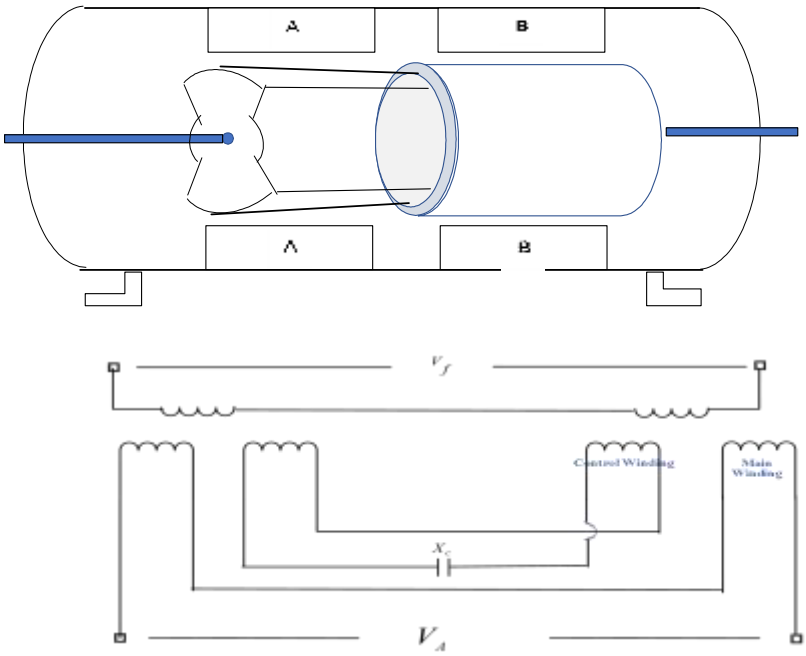


Figure 1: Schematic diagram of the machine arrangement including the windings

(a) Two magnetically isolated stator cores (A, B) with deeper slots to accommodate two sets of windings.
(b) A rotor that is cylindrical cum salient.

It is assumed that if the salient-pole section of the rotor is in stack A say, the cylindrical section will be in stack B. The field winding spans both sections of the rotor and there are damper windings in both sections of the rotor as well. There are two sets of identical windings in the stator cores that are known as the main and control windings respectively. The two windings are electrically isolated but magnetically coupled and their corresponding phases occupy the same slots. The axes of the main windings are the same in both stacks(A,B) and their terminals connected to utility supply whilst the control winding axes are transposed in passing from stack A to B and the terminals connected to a variable capacitor bank. The role of the two windings can be interchanged without any change in performance. Figure 2 shows the exploded view of the rotor in 3-dimensions.

ISSN (online): 2645-2685; ISSN (print): 2756-6811

Figure 2: The exploded rotor view.

### 2.1 Basic Theory of Operation

It is assumed that the salient part of the hybridized rotor is in stack A while the cylindrical part is stack B as shown in Figure 1. When the control winding is on open-circuit, and the pole axis of the salient rotor part is on the direct axis position, the reactance of the main winding on stack A is, $x_d$. In stack B, the reactance is $x_s$ (synchronous reactance) which is made equal to $x_d$ by the adjustment of the air-gaps of the salient and the cylindrical parts.

The total direct axis reactance of the winding $TX_D = X_d + X_d = 2X_d$. When the pole axis of the anisotropic rotor is in the quadrature axis position, the reactance of the main winding in stack A is $x_q$, giving a total quadrature axis reactance $TX_q = X_d + X_q$. The saliency ratio of the machine is thus

$$\frac{TX_D}{TX_Q} = \frac{2X_d}{X_d + X_q} = \frac{2h}{h+1} \tag{1}$$

where $h = \frac{X_d}{X_q}$ is the saliency ratio of the salient-part of the rotor.

For a fixed machine geometry, it is shown in section 4.1 that when the control winding is closed, that the quadrature axis reactance $X_q$ is modified by the capacitive reactance of the control winding while the direct axis reactance remains unaffected. By varying the capacitive reactance, the quadrature axis reactance of the machine becomes variable and can be varied from zero to infinity.

### 2.2 Mathematical Model of The Hybrid Synchronous Machine

The approach used in developing the mathematical model of this hybrid machine is based on the modelling of synchronous machine as contained in literature [8], [9] with due attention given to the peculiar stator configuration of this machine.

In this model, the following assumptions and approximations were adopted:

i. The stator and rotor windings are sinusoidally distributed.
ii. The two stator windings are identical and wound for the same number of poles
iii. The main and control windings of the stator are electrically isolated but magnetically coupled.
iv. The two stacks of the machine are magnetically isolated.
v. Both the main and control windings occupy the same slots (phase by phase).

#### 1) Stator Voltage Equation

The stator voltage equation of the hybrid machine is given by

$$v_{mcr} = i_{mcr} r_{mcr} + \frac{d\lambda_{mcr}}{dt} \tag{2}$$

where $v_{mcr}$ represents the stator (main and control) and the rotor winding voltages. The expanded form of Equation (2) is given in matrix form as Equation (3) and (4);

$$\begin{cases} v_{mcr} = \begin{bmatrix} v_m & v_c & v_r \end{bmatrix} = \begin{bmatrix} v_{ma} & v_{mb} & v_{mc} & v_{ca} & v_{cb} & v_{cc} & v_{qr} & v_{dr} & v_{fr} \end{bmatrix} \\ i_{mcr} = \begin{bmatrix} i_m & i_c & i_r \end{bmatrix} = \begin{bmatrix} i_{ma} & i_{mb} & i_{mc} & i_{ca} & i_{cb} & i_{cc} & i_{qr} & i_{dr} & i_{fr} \end{bmatrix} \\ r_{mcr} = \begin{bmatrix} r_m & r_c & r_r \end{bmatrix} = diag\begin{bmatrix} r_{ma} & r_{mb} & r_{mc} & r_{ca} & r_{cb} & r_{cc} & r_{qr} & r_{dr} & r_{fr} \end{bmatrix} \end{cases} \tag{3}$$

while the flux linkage is given by

$$\lambda_{mcr}=\begin{bmatrix}\lambda_{m_{abc}}\\ \lambda_{c_{abc}}\\ \lambda_{qdr}\end{bmatrix}=\begin{bmatrix}L_{11} & L_{12} & L_{13}\\ L_{21} & L_{22} & L_{23}\\ L_{31} & L_{32} & L_{33}\end{bmatrix}\begin{bmatrix}i_{m_{abc}}\\ i_{c_{abc}}\\ i_{qdr}\end{bmatrix}=\begin{bmatrix}L_{m_{abc}} & L_{m_{abc}c_{abc}} & L_{m_{abc}qdr}\\ L_{c_{abc}m_{abc}} & L_{c_{abc}} & L_{c_{abc}qdr}\\ L_{qdrm_{abc}} & L_{qdrc_{abc}} & L_{qdr}\end{bmatrix}\begin{bmatrix}i_{m_{abc}}\\ i_{c_{abc}}\\ i_{qdr}\end{bmatrix} \tag{4}$$

Equation (5) is obtained from Equation (4),

$L_{m_{abc}}$ is the sum of the $3\times3$ inductance matrix of the three-phase main windings of both stacks of the machine.

$$\therefore L_{m_{abc}}=L_{cr}+L_{ncr} \tag{5}$$

where $L_{cr}$ is the inductance matrix of stack B (cylindrical rotor part) while $L_{ncr}$ is for the stack A (non-cylindrical rotor part). The inductance matrix for the stator winding of any salient pole machine is well known in literature[9] [8] and it is given as Equation (6),

$$L_{ncr}=\begin{bmatrix}L_{ls}+L_o-L_m\cos 2\theta_r & -\frac{1}{2}L_o-L_m\cos 2(\theta_r-\frac{\pi}{3}) & -\frac{1}{2}L_o-L_m\cos 2(\theta_r+\frac{\pi}{3})\\ -\frac{1}{2}L_o-L_m\cos 2(\theta_r-\frac{\pi}{3}) & L_{ls}+L_o-L_m\cos 2(\theta_r-\frac{2\pi}{3}) & -\frac{1}{2}L_o-L_m\cos 2(\theta_r+\pi)\\ -\frac{1}{2}L_o-L_m\cos 2(\theta_r+\frac{\pi}{3}) & -\frac{1}{2}L_o-L_m\cos 2(\theta_r+\pi) & L_{ls}+L_o-L_m\cos 2(\theta_r+\frac{2\pi}{3})\end{bmatrix} \tag{6}$$

where

$$L_o=\frac{1}{3}(L_{md}+L_{mq})\ and\ L_m=\frac{1}{3}(L_{md}-L_{mq}) \tag{7}$$

In the cylindrical stack of the machine stator, the air-gap is uniform and so $L_{md}=L_{mq}$. From Equation(7), $L_o=(2/3)L_{md}$ and $L_m=0$, and the inductance matrix is thus reduced to Equation (8) and (9):

$$\therefore L_{cr}=\begin{bmatrix}L_{ls}+\frac{2}{3}L_{md} & -\frac{1}{3}L_{md} & -\frac{1}{3}L_{md}\\ -\frac{1}{3}L_{md} & L_{ls}+\frac{2}{3}L_{md} & -\frac{1}{3}L_{md}\\ -\frac{1}{3}L_{md} & -\frac{1}{3}L_{md} & L_{ls}+\frac{2}{3}L_{md}\end{bmatrix} \tag{8}$$

$$\therefore L_{m_{abc}}=L_{ncr}+L_{cr}=\begin{bmatrix}2L_{ls}+L_1-L_m\cos 2\theta_r & -L_2-L_m\cos 2(\theta_r-\frac{\pi}{3}) & -L_2-L_m\cos 2(\theta_r+\frac{\pi}{3})\\ -L_2-L_m\cos 2(\theta_r-\frac{\pi}{3}) & 2L_{ls}+L_1-L_m\cos 2(\theta_r-\frac{2\pi}{3}) & -L_2-L_m\cos 2(\theta_r+\pi)\\ -L_2-L_m\cos 2(\theta_r+\frac{\pi}{3}) & -L_2-L_m\cos 2(\theta_r+\pi) & 2L_{ls}+L_1-L_m\cos 2(\theta_r+\frac{2\pi}{3})\end{bmatrix} \tag{9}$$

where;

$$L_1=L_{md}+\frac{1}{3}L_{mq}\ and\ L_2=\frac{1}{2}L_{md}+\frac{1}{6}L_{mq} \tag{10}$$

Also, $L_{m_{abc}c_{abc}}$ is the sum of the $3\times3$ inductance matrix as a result of the mutual inductance between the main and the control stator windings of the machine. Since the main and control windings are identical, and occupy the same slot positions, the mutual inductance between them are equal, and given as its self-inductance minus the leakage inductance [5]. Therefore, if $L_{Mncr}$ is the mutual inductance of the salient-rotor stack then, $L_{Mncr}=L_{ncr}-L_l$. The cylindrical rotor stack is also given by; $L_{Mcr}=L_{cr}-L_l$.

The control winding of the hybrid machine is transposed across the two machine stacks and as a result, their mutual inductance is positive in one stack and negative in the other [5].

$$\therefore L_{m_{abc}c_{abc}}=L_{cr}-L_l-(L_{ncr}-L_l)=L_{cr}-L_{ncr}$$

$$= \begin{bmatrix} L_3+L_m\cos 2\theta_r & L_4+L_m\cos 2(\theta_r-\frac{\pi}{3}) & L_4+L_m\cos 2(\theta_r+\frac{\pi}{3}) \\ L_4+L_m\cos 2(\theta_r-\frac{\pi}{3}) & L_3+L_m\cos 2(\theta_r-\frac{2\pi}{3}) & L_4+L_m\cos 2(\theta_r+\pi) \\ L_4+L_m\cos 2(\theta_r+\frac{\pi}{3}) & L_4+L_m\cos 2(\theta_r+\pi) & L_3+L_m\cos 2(\theta_r-\frac{2\pi}{3}) \end{bmatrix} \quad (11)$$

where,

$$L_3=\frac{L_{md}-L_{mq}}{3} \quad and \quad L_4=\frac{L_{mq}-L_{md}}{6} \quad (12)$$

Also, $L_{m_{abc}qdr}$ is the sum of the mutual inductances between main stator and rotor windings of the two stacks of the machine.

$$\therefore L_{m_{abc}qdr}=\left[L_{m_{abc}qdr}\right]_{cr}+\left[L_{m_{abc}qdr}\right]_{ncr}$$

$$= \begin{bmatrix} (L_{md}+L_{mq})\cos\theta_r & 2L_{md}\sin\theta_r & 2L_{md}\,\mathrm{Sin}\,\theta_r \\ (L_{md}+L_{mq})\cos(\theta_r-\frac{2\pi}{3}) & 2L_{md}\sin(\theta_r-\frac{2\pi}{3}) & 2L_{md}\,\mathrm{Sin}(\theta_r-\frac{2\pi}{3}) \\ (L_{md}+L_{mq})\cos(\theta_r+\frac{2\pi}{3}) & 2L_{md}\sin(\theta_r+\frac{2\pi}{3}) & 2L_{md}\,\mathrm{Sin}(\theta_r+\frac{2\pi}{3}) \end{bmatrix} \quad (13)$$

Since the main and the control windings are identical and occupy the same slot position, then

$$\begin{cases} L_{c_{abc}m_{abc}} = (L_{m_{abc}c_{abc}})^T \\ L_{c_{abc}} = L_{m_{abc}} \\ L_{qdrm_{abc}}=\left(L_{m_{abc}qdr}\right)^T \\ L_{qdrc_{abc}}=\left(L_{c_{abc}qdr}\right)^T \end{cases} \quad (14)$$

Since the control winding is transposed across the two machine stacks, the mutual inductance between the control winding and the rotor winding is the algebraic sum of the mutual inductances of the two machine stacks.

$$L_{c_{abc}qdr} = \left[L_{c_{abc}qdr}\right]_{cr}-\left[L_{c_{abc}qdr}\right]_{ncr}$$

$$= \begin{bmatrix} (L_{md}-L_{mq})\cos\theta_r & 0 & 0 \\ (L_{md}-L_{mq})\cos(\theta_r-\frac{2\pi}{3}) & 0 & 0 \\ (L_{md}-L_{mq})\cos(\theta_r+\frac{2\pi}{3}) & 0 & 0 \end{bmatrix} \quad (15)$$

Also, $L_{qdr}$ is the self-inductance of the rotor winding of the hybrid machine and it is equal to the summation of self-inductance of the two machine stacks. It is given as;

$$L_{qdr}=\left[L_{qdr}\right]_{cr}+\left[L_{qdr}\right]_{ncr}= \begin{bmatrix} L_{lq}+L_{mq}+L_{ld}+L_{md} & 0 & 0 \\ 0 & 2(L_{ld}+L_{md}) & 2L_{md} \\ 0 & 2L_{md} & 2(L_{lf}+L_{md}) \end{bmatrix} \quad (16)$$

It can be seen from Equation (9), (11) and (13) that the inductance of the hybrid synchronous machine has some components that are rotor position dependent and therefore, there is need for transformation using the transformation matrix of Equation (17) to get rid of the rotor position dependent functions.

$$T_{qdo}(\theta_r)=\frac{2}{3}\begin{bmatrix} \cos\theta_r & cos(\theta_r-\frac{2\pi}{3}) & cos(\theta_r+\frac{2\pi}{3}) \\ sin\theta_r & \sin(\theta_r-\frac{2\pi}{3}) & \sin(\theta_r+\frac{2\pi}{3}) \\ \frac{1}{2} & \frac{1}{2} & \frac{1}{2} \end{bmatrix} \quad (17)$$

ISSN (online): 2645-2685; ISSN (print): 2756-6811

Therefore, applying Equations (17) to (9), (11) and (13), the transformed flux linkage equations are given by Equation (18) and (19)

$$\begin{bmatrix} \lambda_{Qs} \\ \lambda_{qs} \\ \lambda_{qcg} \end{bmatrix} = \begin{bmatrix} 2L_{ls}+L_{md}+L_{mq} & L_{md}-L_{mq} & L_{md}+L_{mq} \\ L_{md}-L_{mq} & 2L_{ls}+L_{md}+L_{mq} & L_{md}-L_{mq} \\ L_{md}+L_{mq} & L_{md}-L_{mq} & L_{ld}+L_{lq}+L_{md}+L_{mq} \end{bmatrix} \begin{bmatrix} i_{Qs} \\ i_{qs} \\ i_{qcg} \end{bmatrix} \tag{18}$$

$$\begin{bmatrix} \lambda_{Ds} \\ \lambda_{ds} \\ \lambda_{dcg} \\ \lambda_{df} \end{bmatrix} = \begin{bmatrix} 2(L_{ls}+L_{md}) & 0 & 2L_{md} & 2L_{md} \\ 0 & 2(L_{ls}+L_{md}) & 0 & 0 \\ 2L_{md} & 0 & 2(L_{ld}+L_{md}) & 2L_{md} \\ 2L_{md} & 0 & 2L_{md} & 2(L_{lf}+L_{md}) \end{bmatrix} \begin{bmatrix} i_{Ds} \\ i_{ds} \\ i_{dcg} \\ i_{df} \end{bmatrix} \tag{19}$$

Simplifying equations (18) and (19) gives the flux linkage Equations (20),

$$\begin{cases} \lambda_{Qs}=2L_{ls}i_{Qs}+2L_{mq}i_{Qs}+2L_{mq}i_{qcg}+(L_{md}-L_{mq})(i_{Qs}+i_{qs}+i_{qcg}) \\ \lambda_{Ds}=2L_{ls}i_{Ds}+2L_{md}(i_{Ds}+i_{dcg}+i_{df}) \\ \lambda_{qs}=2L_{ls}i_{qs}+2L_{mq}i_{qs}+(L_{md}-L_{mq})(i_{Qs}+i_{qs}+i_{qcg}) \\ \lambda_{ds}=2L_{ls}i_{ds}+2L_{md}i_{ds} \\ \lambda_{qcg}=(L_{ld}+L_{lq})i_{qcg}+2L_{mq}i_{qcg}+2L_{mq}i_{Qs}+(L_{md}-L_{mq})(i_{Qs}+i_{qs}+i_{qcg}) \\ \lambda_{dcg}=2L_{ld}i_{dcg}+2L_{md}(i_{Ds}+i_{dcg}+i_{df}) \\ \lambda_{df}=2L_{lf}i_{df}+2L_{md}(i_{Ds}+i_{dcg}+i_{df}) \end{cases} \tag{20}$$

From Equation(19), it is seen that the overall d-axis inductances are completely decoupled from the q-axis inductances whereas there is a coupling term between the d and q axes inductances in the overall q-axis inductance of Equation (18). This explains why the d-axis inductance is independent of the variation of the capacitor bank in the control winding.

**2) The qdo Voltage Equation**

The voltage equation in machine variable is given as Equation (21);

$$v_{abc}=2r_s i_{abc}+p\lambda_{abc} \tag{21}$$

These machine variables can be transformed to qdo [8].

$$v_{qdo} = T_{qdo}r_s T_{qdo}^{-1} i_{qdo} + T_{qdo}PT_{qdo}^{-1}\lambda_{qdo} \tag{22}$$

Simplifying this gives Equation (23)

$$v_{qdo}=2r_s i_{qdo}+\omega_r \begin{bmatrix} 0 & 1 & 0 \\ -1 & 0 & 0 \\ 0 & 0 & 0 \end{bmatrix} \lambda_{qdo}+p\lambda_{qdo} \tag{23}$$

Simplifying Equation (23) and representing main winding components with capital letters while representing control winding components with small letters, gives Equation (24)

$$\begin{cases} V_{Qs}=2r_s i_{Qs}+\omega_r\lambda_{Ds}+p\lambda_{Qs} \\ V_{Ds}=2r_s i_{Ds}-\omega_r\lambda_{Qs}+p\lambda_{Ds} \\ V_{Os}=2r_s i_{Os}+p\lambda_{Os} \\ V_{qs}=2r_s i_{qs}+\omega_r\lambda_{ds}+p\lambda_{qs}+v_{cq} \\ V_{ds}=2r_s i_{ds}-\omega_r\lambda_{qs}+p\lambda_{ds}+v_{cd} \\ V_{os}=2r_s i_{os}+p\lambda_{os}+v_{co} \\ V_{qcg}=2r_{cg}i_{qcg}+p\lambda_{qcg}=0 \\ V_{dcg}=2r_{cg}i_{dcg}+p\lambda_{dcg}=0 \\ V_{df}=2r_{df}I_{df}+p\lambda_{df} \end{cases} \tag{24}$$

ISSN (online): 2645-2685; ISSN (print): 2756-6811

The q-axis and d-axis dynamic equivalent circuits of the hybrid machine are drawn using Equations (20) and (24) are shown in Figures 3 and 4 respectively.

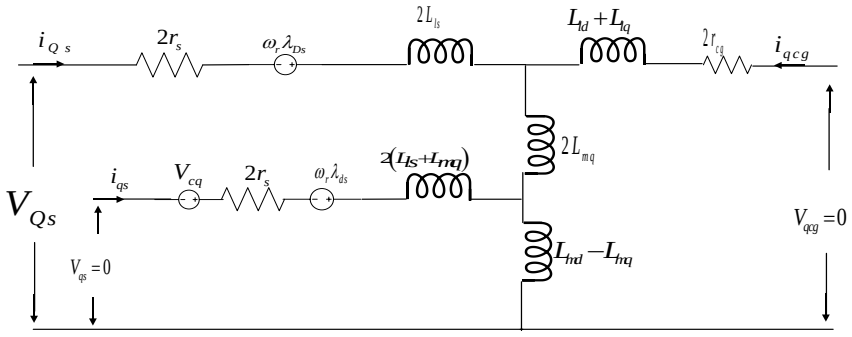


Figure 3: Q – axis equivalent circuit of the hybrid synchronous machine

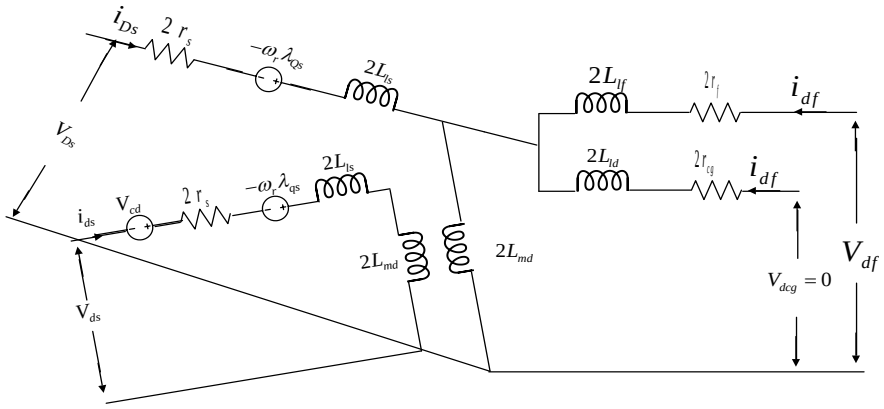


Figure 4: D-Axis equivalent circuit of the hybrid synchronous machine

**3) Capacitor Voltage Equation**

The contl winding of this hybrid machine is connected to a balanced capacitor and the current flowing through the winding is given by:

$$i_{c_{abc}} = \frac{d}{dt} q_{c_{abc}} \tag{25}$$

Applying Park's transformation equations to Equation (25) gives Equation (26);

$$i_{qdos} = TP[(T)^{-1} q_{qdos}^{-1}] + T(T)^{-1} P q_{qdos} \tag{26}$$

Since $TP[(T)^{-1}] = \omega_r \begin{bmatrix} 0 & 1 & 0 \\ -1 & 0 & 0 \\ 0 & 0 & 0 \end{bmatrix}$ Then;

$$i_{qdos} = \omega_r \begin{bmatrix} 0 & 1 & 0 \\ -1 & 0 & 0 \\ 0 & 0 & 0 \end{bmatrix} q_{qds} + p q_{qdos} \tag{27}$$

where, $[q_{qds}]^T = [q_{ds}\ q_{qs}\ 0]$

In expanded form

$$i_{qs} = \omega_r q_{ds} + p q_{qs} \tag{28}$$

$$i_{ds} = -\omega_r q_{qs} + p q_{ds} \tag{29}$$

But $q = CV$

Then,

$$i_{qc} = \omega_r C V_{cdc} + C p V_{cqc} \tag{30}$$

$$i_{dc} = -\omega_r C V_{cqc} + C p V_{cdc} \tag{31}$$

Simplifying further,

$$pv_{cq} = \frac{i_{qc}}{C} - \omega_r v_{cd} \tag{32}$$

$$pv_{cd} = \frac{i_{dc}}{C} + \omega_r v_{cq} \tag{33}$$

Since the control winding of this machine is terminated on a balanced capacitor bank, the current in the winding will be the same as the capacitor current. Therefore $i_{qc} = I_{qs}$ *and* $i_{dc} = I_{ds}$ as in Equation (32) and (33).

### 2.3 The Electromagnetic Torque

The total input power to the machine in machine variable is given as Equation (34);

$$P_{abc} = v_{As} i_{As} + v_{Bs} i_{Bs} + v_{Cs} i_{Cs} + v_{as} i_{as} + v_{bs} i_{bs} + v_{cs} i_{cs} + V_f I_f \tag{34}$$

Transforming the power to rotor reference frame using Park's equation gives

$$P_{qdo} = v_{qdo}^T (T^{-1})^T (T^{-1}) i_{qdo}$$

where $(T^{-1})^T (T^{-1}) = \frac{3}{2}\begin{bmatrix} 1 & 0 & 0 \\ 0 & 1 & 0 \\ 0 & 0 & 2 \end{bmatrix}$

Therefore

$$P_{qdo} = \frac{3}{2}(v_{Qs} i_{Qs} + v_{Ds} i_{Ds} + 2v_{Os} i_{Os} + v_{qs} i_{qs} + v_{ds} i_{ds} + 2v_{os} i_{os} + V_f I_f) \tag{35}$$

The expression for the electromagnetic torque can be derived using power balance equation of the machine. The zero sequence currents $I_{Os}$ *and* $I_{os}$ are usually zero, and hence the instantaneous power, $P_{in}$ flowing into the machine can be written from the $dq$ frame variable as

$$P_{in} = \frac{3}{2}(v_{Qs} i_{Qs} + v_{Ds} i_{Ds} + v_{qs} i_{qs} + v_{ds} i_{ds} + V_f I_f) \tag{36}$$

Substituting Equation (24) into Equation (36) gives Equation (37),

$$P_{in} = \frac{3}{2}\left\{\begin{array}{l} \underbrace{(r_s(i_{Ds}^2 + i_{Qs}^2 + i_{ds}^2 + i_{qs}^2) + r_f I_f^2}_{\text{Power loss}} + \underbrace{\omega_r(\lambda_{Ds} i_{Qs} - \lambda_{Qs} i_{Ds}) + \omega_r(\lambda_{ds} i_{qs} - \lambda_{qs} i_{ds})}_{\text{Energy conversion}} + \\ \underbrace{i_{Ds} p\lambda_{Ds} + i_{Qs} p\lambda_{Qs} + i_{ds} p\lambda_{ds} + i_{qs} p\lambda_{qs} + I_f p\lambda_f}_{\text{Energy stored}} + \underbrace{v_{cd} i_{ds} + v_{cq} i_{qs}}_{\text{Energy stored in capacitor}} \end{array}\right\} \tag{37}$$

From Equation(37), the second term is the part that indicates the electrical to mechanical energy conversion. Therefore, the electromagnetic power is given as Equation (38).

$$P_{em} = \frac{3}{2}[\omega_r(\lambda_{Ds} i_{Qs} - \lambda_{Qs} i_{Ds}) + \omega_r(\lambda_{ds} i_{qs} - \lambda_{qs} i_{ds})] \tag{38}$$

For a P-pole machine, $\omega_r = (\frac{P}{2})\omega_{rm}$;

where $\omega_{rm}$ is the rotor speed in mechanical radians per second. Thus, for a P-pole machine, Equation (38) can be written as Equation (39)

$$P_{em} = \frac{3}{2}\frac{P}{2}\omega_{rm}\{(\lambda_{Ds} i_{Qs} - \lambda_{Qs} i_{Ds}) + (\lambda_{ds} i_{qs} - \lambda_{qs} i_{ds})\} \tag{39}$$

The electromagnetic torque is given as Equation (40);

$$T_{em}=\frac{3}{2}\frac{P}{2}\left\{(\lambda_{Ds}i_{Qs}-\lambda_{Qs}i_{Ds})+(\lambda_{ds}i_{qs}-\lambda_{qs}i_{ds})\right\} \tag{40}$$

Substituting Equation (20) into Equation (40), gives Equation (41)

$$T_{em}=\frac{3}{2}\frac{P}{2}\left\{\underbrace{\left(L_{md}-L_{mq}\right)i_{Ds}i_{Qs}+\left(L_{md}-L_{mq}\right)i_{ds}i_{qs}+\left(L_{md}-L_{mq}\right)\left(i_{qs}i_{Ds}+i_{Qs}i_{ds}\right)}_{\text{Reluctance Torque}}+\underbrace{2L_{md}I_{df}i_{Qs}}_{\text{Excitation Torque}}\underbrace{+2L_{md}i_{dcg}i_{Qs}-2L_{mq}i_{qcg}i_{Ds}-\left(L_{md}-L_{mq}\right)\left(i_{qcg}i_{Ds}+i_{qcg}i_{ds}\right)}_{\text{Induction Torque}}\right\} \tag{41}$$

From Equation(41), it can be seen that the electromagnetic output torque of this hybrid machine has three major components.

The first component is the reluctance torque. This reluctance torque can be seen to comprise three components which are;

i. Reluctance torque due to the stator main winding.

$$T_{r1}=\frac{3}{2}\frac{P}{2}\left(L_{md}-L_{mq}\right)i_{Ds}i_{Qs} \tag{42}$$

ii. Reluctance torque due to the stator control winding

$$T_{r2}=\frac{3}{2}\frac{P}{2}(L_{md}-L_{mq})i_{ds}i_{qs} \tag{43}$$

iii. Reluctance torque due to the interaction between the stator main and control winding

$$T_{r3}=\frac{3}{2}\frac{P}{2}\left(L_{md}-L_{mq}\right)\left(i_{Ds}i_{qs}+i_{Qs}i_{ds}\right) \tag{44}$$

These reluctance torque components are affected by the variation of the value of the capacitor at the control winding. Here the q-axis inductances are affected by the variation of the capacitor value while the d-axis inductance is not affected by the variation.

The second component is the excitation torque. This torque is as a result of the field excitation. The third component is the induction torque. This component of the torque vanishes once the machine attains the synchronous speed and it is as a result of the interaction between the stator windings and the caged windings.

The rotational motion of the motor is

$$\begin{cases}P\omega_r=(T_e-T_L)/J\\ \theta_r=\int\omega_r dt\end{cases} \tag{45}$$

where, $J$ is the moment of inertia, $T_L$ is the load torque and $\omega_r$ is the rotor mechanical speed.

### 2.4 Dynamic Performance Analysis of the Hybrid Machine

The dynamic performance analysis of this hybrid synchronous machine is carried out using the parameters of a 4-pole, 5kW, 220V, 50Hz, 3-phase line-start salient-pole synchronous machine. The unsaturated inductances of the machine are: $L_{md}=0.0211H$ , $L_{mq}=0.0182H$ , $L_{ls}=0.00095H$ , $L_{lfr}=0.0009H$ , $L_{ldr}=L_{lqr}=0.001375H$ , $r_s=1.05\Omega$ and $r_{lfr}=21\Omega$.

The effect of saturation was confined to the direct axis and did not affect the quadrature axis and given by the polynomial curve fits. These parameters are expressed as a function of the flux linkages and used to adjust the direct axis inductance and are given as [10], [11]

$$L_d=0.221e^{(-0.91i_s+0.21i_s^2-0.025i_s^3)}H \tag{46}$$

The magnetic flux due to the field excitation is assumed not to have been affected by the saturation.

## 3. RESULTS AND DISCUSSIONS

The dynamic performance characteristics of the hybrid synchronous machine was carried out in MATLAB/Simulink environment using the characteristic equation derived in section 2. The performance analysis is done under step loading and ramp loading. Figures 4 to 13 show the simulation resuls under step load. The speed/time characteristics of the machine is shown in Figure 4. Just like a conventional synchronous machine, its speed bulds from zero to synchronous speed.

ISSN (online): 2645-2685; ISSN (print): 2756-6811

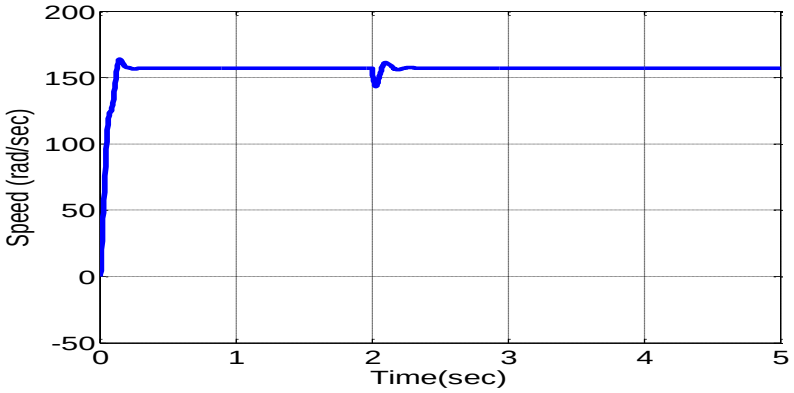


Figure 4: Speed-time characteristics of the machine

It was shown in Equation (41) that the output electromagnetic torque of this machine comprises three components, which are; the reluctance torque, excitation torque, and the induction motor torque. The plots of the different components of the output torque of the hybrid machine are shown in Figures 5 to 8.

The first component of the electromagnetic torque which is the reluctance torque also comprises three components as shown in Equations(42), (43) and (44). The comparative view of the total reluctance components is shown in Figure 5. It can be seen that the reluctance torque due to the main winding is highest, followed by that due to the interaction between the main and the auxiliary winding. The reluctance torque due to the auxiliary winding is the least. This can be attributed to the fact that the current in the auxiliary winding is due to the capacitor connect to it and subsequently, the flux due to the current in the auxiliary winding is small.

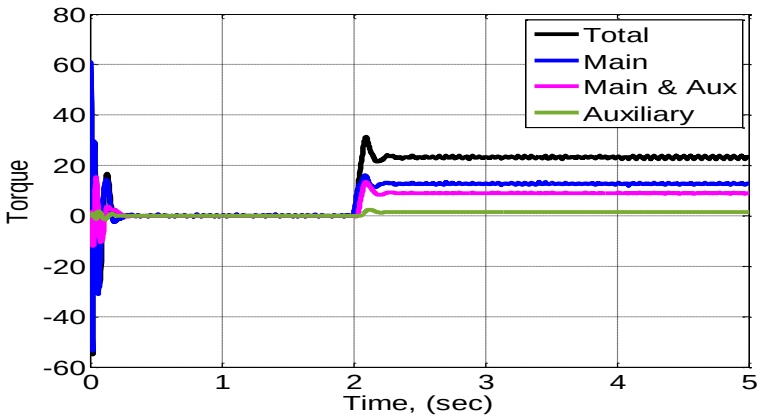


Figure 5: Total reluctance torque of the hybrid machine

The third component of the torque is the induction motor torque which is as a result of the induced voltage on the damper at starting. It becomes zero at synchronous speed. The two torque components of a typical synchronous machine are the excitation and the reluctance torque. The comparative view of the excitation and the reluctance torque is shown in Figure 6. It is shown that unlike the conventional synchronous machine, the reluctance torque is higher than the excitation torque. The value of the reluctance toque could be increased further by varying the capacitor on the control winding.

ISSN (online): 2645-2685; ISSN (print): 2756-6811

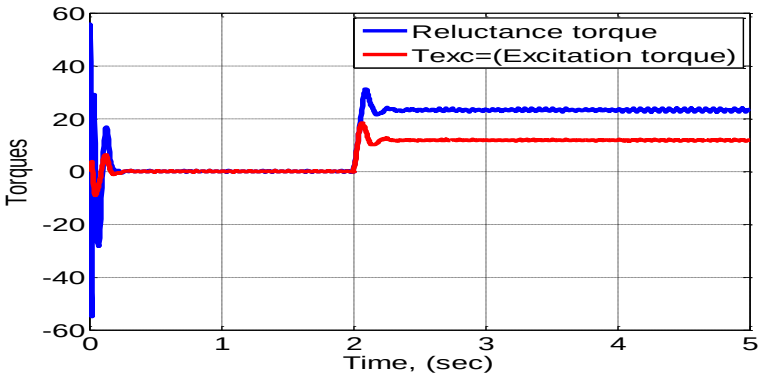


Figure 6: Comparative view of the reluctance and excitation torque

The currents in the main and the control windings are shown in Figures 7 and 8. It can be seen from the figure that at no-load, the current in the control winding is approximately zero. The current drawn in the main winding indicates the machine performance is at the rated power.

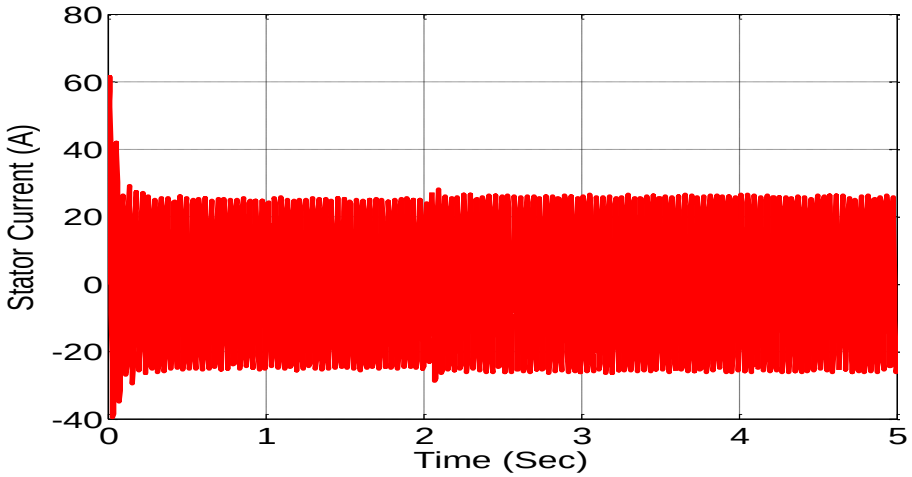


Figure 7: Main winding stator current (phase A) of the hybrid synchronous machine

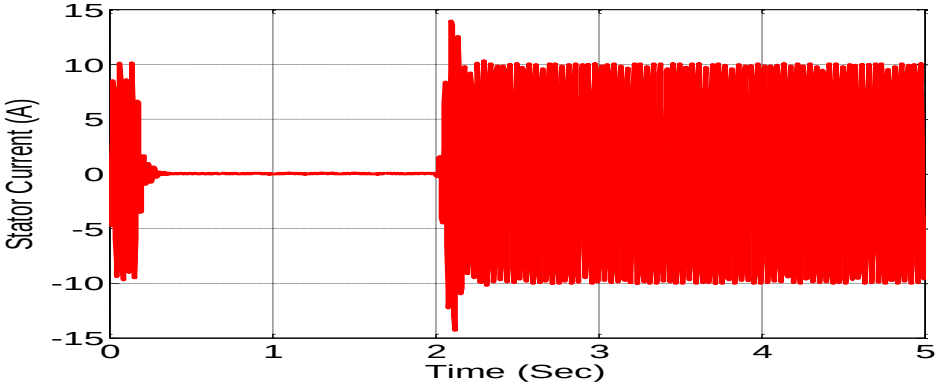


Figure 8: Control winding stator current (phase a) of the hybrid synchronous machine

The loading capability of the hybrid machine is investigated under ramp loading. The simulation results of the performance of the machine under ramp loading are shown in Figures 9. The loading capability of a machine shows the maximum load the machine can support under over-load condition. A conventional synchronous machine of the same rating can support a load torque of 20Nm while as can be seen from the speed-load characteristics, this hybrid machine can support load torque of 62Nm. This is indeed great improvement.

ISSN (online): 2645-2685; ISSN (print): 2756-6811

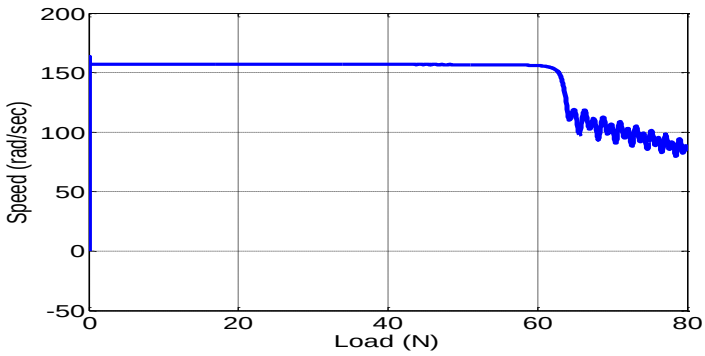


Figure 9: Speed – load characteristic of the hybrid synchronous machine under ramp load

## 4. CONCLUSION

The mathematical modelling and dynamic analysis of a hybrid synchronous machine has been carried out. The machine, though having a salient cum cylindrical rotor, operates like a salient-pole synchronous machine. It is shown that unlike the conventional synchronous machine, this hybrid machine has a higher reluctance torque than the excitation torque and thus a higher output capability than the conventional type. The machine has a better synchronising characteristic because $TX_D/TX_Q$ ratio can be adjusted very low at synchronisation and thereafter raised higher. The machine can be optimized for wind power application because of its adjustable output power.

## REFERENCES

[1] Lawrenson, P. J. & Agu, L.A. (1964). Theory and performance of polyphase reluctance machines, *Proc. Inst. Electr. Eng.*, 111(8), 1435-1445, doi: 10.1049/piee.1964.0237.
[2] Kostko, J.K. (2013). Polyphase reaction synchronous motors, *J. Am. Inst. Electr. Eng.*, 42(11), 1162–1168, doi: 10.1109/joaiee.1923.6591529.
[3] Lawrenson, P.J. (1965). "Development and application of reluctance motors," *Electron. Power*, 11(6), 195-198, doi: 10.1049/ep.1965.0151.
[4] Cruickshank, A. J. O., Menzies, R. W. & Anderson, A. F. (1966). Axially laminated anisotropic rotors for reluctance motors, *Proc. Inst. Electr. Eng.*, 113(12), 2058-2060, doi: 10.1049/piee.1966.0358.
[5] Anih, L. U. Obe, E. S. & Abonyi, S. E. (2015). Modelling and performance of a hybrid synchronous reluctance machine with adjustable X d / X q ratio," *IET Electr. Power Appl.*, 9(2), 171–182, doi: 10.1049/iet-epa.2014.0149.
[6] Agbachi, E. O., Anih, L. U. & Obe, E. S. (2022). Steady-State Analysis of Hybrid Synchronous Machine With Higher Reluctance to Excitation Power Ratio, *Iran. J. Electr. Electron. Eng.*, 18(1), 1–12, [Online]. Available: ijeee.iust.ac.ir
[7] Agbachi, E. O., Anih, L. U. & Obe, E. S. (2022). Modeling and Dynamic Analysis of hybrid synchronous machine, in *2022 IEEE NIGERCON*, 0–4.
[8] Chee-Mun O. (1998), *Dynamic Simulation of Electric Machinery using Matlab/Simulink*. New Jersey: Printice Hall PTR.
[9] Krause, P. C., Oleg, W. & Scott, S. D. (2002). *Analysis of Electric Machinery and Drive System*, Second. A John Wiley & Sons, Inc. Publication.
10] Ojo, O. & Cox, J. (1996). Investigation into the performance characteristics, *Industry Applications Conference*, 533–540.
[11] Todorov, G. & Stoev, B. (2016). Saturation effects on the parameters of interior permanent magnet synchronous motors with different rotor configuration, *Mater. Sci. Forum*, 856(5), 257–262, doi: 10.4028/www.scientific.net/MSF.856.257.